Proceedings of the ASME 2012 Internal Combustion Engine Division Spring Technical Conference
ICES2012
May 6-9, 2012, Torino, Italy

DRAFT ICES2012-81145

CYCLIC COMBUSTION VARIATIONS IN DUAL FUEL PARTIALLY PREMIXED PILOT-IGNITED NATURAL GAS ENGINES

K.K. Srinivasan[1,†] **S.R. Krishnan[1]** **Y. Qi[2]**

[1]Department of Mechanical Engineering, Mississippi State University, MS 39762
[2]Caterpillar, Inc., Peoria, IL
[†]Corresponding Author: srinivasan@me.msstate.edu

ABSTRACT

Dual fuel pilot ignited natural gas engines are identified as an efficient and viable alternative to conventional diesel engines. This paper examines cyclic combustion fluctuations in conventional dual fuel and in dual fuel partially premixed low temperature combustion (LTC). Conventional dual fueling with 95% (energy basis) natural gas (NG) substitution reduces NOx emissions by almost 90%t relative to straight diesel operation; however, this is accompanied by 98% increase in HC emissions, 10 percentage points reduction in fuel conversion efficiency (FCE) and 12 percentage points increase in COVimep. Dual fuel LTC is achieved by injection of a small amount of diesel fuel (2-3 percent on an energy basis) to ignite a premixed natural gas–air mixture to attain very low NOx emissions (less than 0.2 g/kWh). Cyclic variations in both combustion modes were analyzed by observing the cyclic fluctuations in start of combustion (SOC), peak cylinder pressures (Pmax), combustion phasing (Ca50), and the separation between the diesel injection event and Ca50 (termed "relative combustion phasing"). For conventional dual fueling, as % NG increases, Pmax decreases, SOC and Ca50 are delayed, and cyclic variations increase. For dual fuel LTC, as diesel injection timing is advanced from 20° to 60°BTDC, the relative combustion phasing is identified as an important combustion parameter along with SoC, Pmax, and CaPmax. For both combustion modes, cyclic variations were characterized by alternating slow and fast burn cycles, especially at high %NG and advanced injection timings. Finally, heat release return maps were analyzed to demonstrate thermal management strategies as an effective tool to mitigate cyclic combustion variations, especially in dual fuel LTC.

NOMENCLATURE

ALPING	advanced injection low pilot ignited natural gas
ATDC	after top dead center
BMEP	brake mean effective pressure
BTDC	before top dead center
CAD	crank angle degrees
Ca50	crank angle corresponding to 50% mass burn
CaPmax	crank angle at which Pmax occurs
CO	carbon monoxide
CO_2	carbon dioxide
COVimep	coefficient of variation of IMEP
EGR	exhaust gas recirculation
FCE	fuel conversion efficiency
HC	total hydrocarbons (brake-specific)
IMEP	indicated mean effective pressure
LTC	low temperature combustion
$\dot{m}_d$	mass flow rate of diesel
NG	natural gas
NOx	oxides of nitrogen (brake-specific)
P_{in}	intake boost pressure
Pmax	maximum pressure in engine cycle
PM	particulate matter
RCCI	reactivity controlled compression ignition
SEC	specific energy consumption
SOC	start of combustion
SOI	start of injection of pilot diesel fuel
T_{in}	intake temperature
TDC	top dead center
Φ	fuel-air equivalence ratio

1. INTRODUCTION

Emissions regulations and fuel conversion efficiency requirements for future internal combustion engines, coupled with the need to find sustainable alternatives for fossil fuels, have driven the search for cleaner, more efficient combustion strategies. Dual fuel combustion [1], which has been employed in stationary engines for several decades, has received renewed interest in both heavy-duty and light-duty transportation engines. The primary benefits of dual fuel combustion include "diesel-like" fuel conversion efficiencies and low emissions of oxides of nitrogen (NOx) and particulate matter (PM). In response to increasingly restrictive emissions standards and fuel

efficiency requirements, dual fuel combustion has continued to evolve over the past few decades.

Figure 1 is a plot of specific NOx versus specific energy consumption (SEC) for selected dual fuel combustion strategies available in the open literature. These quantities were computed based on the experimental data reported in the respective references and represent either "brake" or "indicated" values. As evident from Fig. 1, dual fuel technologies have progressed over the last 15 years in meeting or surpassing the well known efficiency-emissions tradeoff paradigm. Of particular merit is the fact that the engine-out NOx values reported were obtained by solely relying on in-cylinder control strategies with no exhaust aftertreatment. Classical dual fuel combustion involves the induction of a primary high-octane gaseous fuel (e.g., natural gas) with the intake air, forming a lean premixed fuel-air mixture that is highly resistant to autoignition. This mixture is ignited by direct injection of a high-cetane liquid fuel (e.g., diesel) toward the end of the compression process. For example, in classical diesel-ignited natural gas (NG) dual fuel combustion, the energy release can be considered to occur in three distinct phases [1]. The first phase involves energy release from the combustion of the diesel pilot; the second arises due to combustion of natural gas in the vicinity of the diesel pilot; and the third from flame propagation in the lean natural gas–air mixture.

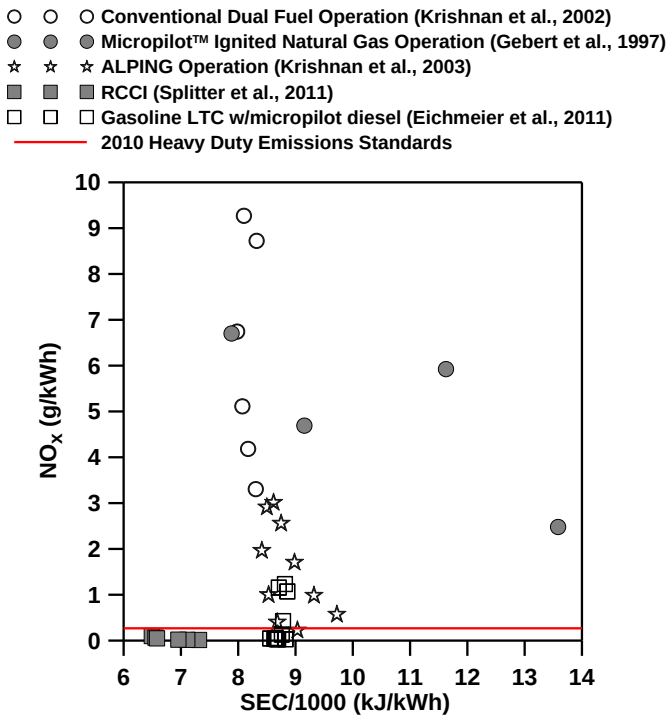

Figure 1: Progression of dual fuel combustion strategies in achieving good fuel efficiencies and low engine-out NOx emissions

Several investigations on dual fuel NG technologies confirm their potential to reduce NOx emissions over a wide range of engine conditions. However, these benefits are accompanied by fuel conversion efficiency and hydrocarbon emissions penalties, particularly at low loads [2-4]. Also, it is well documented that NOx emissions scale with diesel pilot sizes [2-5]. This implies that dual fuel NOx emissions are reduced by decreasing the amount of diesel used (i.e., at high NG substitutions). Therefore, the performance and emissions benefits from conventional dual fuel engines were limited in the past by the turndown ratio of the mechanical diesel injection systems. The advent of electronic diesel fuel injection systems in the late 1990s to meet stringent emissions statutes refocused attention on dual fueling. For instance, as indicated in Fig. 1, the potential for diesel-like fuel conversion efficiencies with simultaneous reduction in engine-out NOx emissions was demonstrated using very small diesel pilots by Gebert et al. [6] with their Micropilot™ technology.

Krishnan et al. [7] (see Fig. 1) and Srinivasan et al. [8] demonstrated that ultra-low engine-out NOx emissions (less than 0.2 g/kWh without any exhaust aftertreatment) with diesel-equivalent fuel conversion efficiencies (about 40 percent) were possible with the Advanced injection Low Pilot Ignition Natural Gas (ALPING) dual fuel combustion strategy. The ALPING combustion concept employs very early injection (approximately 60°BTDC) of small diesel pilots (1-5 percent on an energy basis) to ignite lean premixed natural gas-air mixtures (overall equivalence ratios ranging from 0.25 – 0.6). The early injection of diesel results in "sufficient" residence time for the diesel fuel to form distributed ignition sites. It is hypothesized that combustion begins at these dispersed ignition sites and consumes the unburned lean premixed natural gas-air mixture by localized flame propagation. The presence of multiple ignition sites and the occurrence of partially premixed low temperature combustion (LTC) result in high fuel conversion efficiencies and ultra-low NOx emissions. More recently, Splitter et al. [9] have demonstrated the Reactivity Controlled Compression Ignition (RCCI) dual fuel combustion concept. The RCCI concept uses diesel sprays to ignite premixed gasoline-air mixtures to ensure optimal in-cylinder blending of diesel and gasoline to control the overall combustion process and realize indicated efficiencies well above 50 percent and very low NOx emissions. It must be noted that the reported indicated fuel conversion efficiencies in Ref. [9] are much higher than possible with state-of-the-art diesel engines and the indicated specific NOx (isNOx) emissions are well below 2010 statutes. The most recent demonstration of micropilot technology was by Eichmeier et al. [10], who used very small diesel pilots injected early in the compression stroke to ignite premixed gasoline-air mixtures. They were also able to obtain diesel-like (or sometimes higher) fuel conversion efficiencies with simultaneous reduction in NOx emissions. As shown in Fig. 1, the diesel-ignited gasoline LTC concept of Ref. [10] has NOx-SEC benefits similar to ALPING combustion demonstrated by Krishnan et al. [7].

In summary, dual fuel combustion technologies offer immense potential in overcoming the NOx-smoke and NOx-fuel conversion efficiency (or SEC) tradeoffs encountered by modern diesel engines. In this paper, we attempt to describe the nature of cyclic combustion variations associated with pilot

ignited natural gas dual fuel combustion concepts. We believe that this study is warranted given the present resurgence of natural gas as a viable alternative to fossil fuels.

2. EXPERIMENTAL SETUP

The experiments were performed on a single-cylinder research engine (see Table 1 for engine specifications). The engine was coupled to a DC dynamometer through a torque meter. Intake, exhaust, coolant, and oil temperatures were measured using Type-K thermocouples. To simulate turbocharging, compressed inlet air was heated in a surge-tank and fed to the intake manifold while the exhaust back pressure was controlled by regulating the pressure in the exhaust tank. City natural gas was used in all of these experiments and gas composition analysis showed that the natural gas contained predominantly methane (approximately 98.3 percent).

The intake airflow rate and natural gas flow rate were measured using a laminar flow element and a thermal mass flow meter, respectively. The conventional dual fuel experiments were performed using a stock mechanical injection system with a static diesel injection timing of 22°BTDC. The ALPING experiments were performed with pilot injection of diesel fuel using a customized, accumulator-type, electronic common rail injection system, which is capable of consistently metering a minimum injected quantity of 4.6 mm^3/stroke and a maximum injected quantity of 20 mm^3/stroke. Natural gas was fumigated through the intake manifold. Crank resolved pressure data acquired over 150 successive engine cycles were used in a two-zone heat release analysis program [3] to obtain experimental heat release and mass burn rates, the start of combustion (SOC), the crank angle corresponding to 50 percent mass burn (Ca50), amongst others. In this study, the SOC is defined as the crank angle corresponding to 1 percent mass burn.

Table 1: Single cylinder research engine specifications

Parameter	Specification
Engine Type	4-str. simulated turbocharging
Bore × Stroke, mm	137 × 165
Displacement, L	2.43
Compression Ratio	14.5:1
Primary Fuel	Compressed Natural Gas
Gas Supply	Intake Manifold, 206 kPa
Ignition Source	Diesel Pilot, Direct Injection
Diesel Injection System	Electronic, Common Rail
Number of Nozzle Holes	4
Number of Valves	4
Engine Rating	52 kW at 2100 rev/min

The exhaust emissions were measured by an integrated emissions bench. The emissions were sampled near the exhaust port and directed to the emissions bench through a heated sample line. Total hydrocarbons (HC) and NOx were measured in the hot, undried sample using a heated flame ionization detector and a chemiluminescent detector respectively. The exhaust sample was cooled and dried prior to the measurement of O_2, CO and CO_2. The species CO and CO_2 were measured using the non-dispersive infrared method and O_2 was measured by the paramagnetic method in a separate analyzer.

Both the conventional and ALPING dual fuel experiments included the measurement of all gaseous emissions (CO, CO_2, O_2, NOx, and HC) and in-cylinder pressure histories over a wide range of engine operating conditions. The ALPING dual fuel experiments were performed over a wide range of injection timings (20° - 60°BTDC). Both dual fuel and ALPING dual fuel experiments were performed at a constant engine speed of 1700 rev/min at suitable combinations of intake charge temperature (T_{in}), intake pressure (P_{in}), exhaust back pressure (P_{ex}), and diesel flow rates ($\dot{m}_d$). Further details of the experimental matrix reported in this paper can be found in Refs. [3], [7], and [8]. The results reported in this paper correspond to half load conditions (brake power = 21 kW, BMEP = 6 bar), nominal T_{in}=75°C, P_{in}=181 kPa, and P_{ex}=171 kPa for both conventional dual fuel and ALPING dual fuel experiments, with the injected diesel quantity fixed at 3.3 g/min for the ALPING experiments

3. RESULTS AND DISCUSSION

3.1. Conventional Dual Fuel Combustion

Figure 2 shows the brake-specific NOx and HC emissions, the coefficient of variation of indicated mean effective pressure (COVimep), and fuel conversion efficiencies (FCE) versus the relative combustion phasing for various natural gas substitutions at a fixed SOI of 22°BTDC for conventional dual fuel combustion. In this figure, the relative combustion phasing quantifies the separation of the combustion event (as represented by the Ca50) from the diesel injection event (as represented by SOI). Several trade-offs emerge from this plot. For instance, the trade-off between NOx and HC is directly evident. As NG substitution increases, the NOx emissions decrease sharply while the HC emissions increase. The reduction in NOx emissions is likely due to a combination of two phenomena: (i) a reduction in pilot diesel quantity, and (ii) the separation of the diesel pilot injection event from the overall combustion process. As discussed in Ref. [3], the pilot injection duration (not shown here for the sake of brevity) decreases from 20 CAD for straight diesel operation (0% NG) to nearly 6 CAD for 95% NG substitution. Also, the apparent ignition delay (not shown here) increases from 9 CAD for 0% NG to 13.5 CAD for 95% NG substitution. Therefore, it is clear that with increasing NG addition the pilot injection event is increasingly separated from the combustion event (at 95% NG, there is complete separation). This separation implies that as NG substitution is increased, the diesel spray has more time available to disperse into the surrounding NG-air mixture before SOC. As a result, it is progressively less likely for a high-temperature diffusion flame to envelop the diesel spray during combustion, especially at 95% NG. Since most of the NOx emissions form in the high-temperature diffusion flame surrounding diesel sprays [11] (note that the NG-air mixture is

usually too lean to form substantial amounts of NOx), the NOx emissions are quite low at 95% NG compared to 0% NG. On the other hand, at 50% NG, the injection duration is about 14 CAD whereas the apparent ignition delay is about 9.5 CAD. Clearly, the pilot diesel injection event is still occurring after SOC and so there is some overlap between the diesel injection event and the overall combustion event. This indicates that the diesel jet is still existent as the combustion starts; thereby, enabling a high-temperature diffusion flame to envelop the jet and subsequently support NOx formation. Obviously, this phenomenon is more evident in the 0% NG case where the injection event lasts for almost 20 CAD but the combustion begins at 6 CAD after SOI.

Also shown in Fig. 2 is the steep increase in HC emissions with increasing NG substitution, which is attributable to slower combustion rates. The relative combustion phasing is also progressively removed from TDC with increasing NG addition. In particular, for 95% NG, the combustion event is almost 35 CAD away from the SOI. Therefore, most of the combustion process occurs in the expansion stroke during which the bulk cylinder temperature is lower, thereby impeding flame propagation in the already lean premixed NG-air mixture. This results in the expulsion of unburned fuel (as HC emissions) through the exhaust.

Another tradeoff in Fig. 2 is between NOx and FCE. These results show that it is not possible to achieve simultaneous reduction in NOx emissions, while maintaining or exceeding diesel FCEs. The lowering of FCE with increasing NG substitution is caused by the delayed combustion phasing (Ca50), which results in the reduction of cylinder volume available for expansion work. Finally, increasing NG addition also leads to higher cyclic variations as indicated by high COVimep (approximately 12 percent at 95% natural gas substitution). In summary, while conventional dual fuel combustion aids NOx reduction, it introduces other problems such as increased cyclic combustion variations and high unburned HC emissions that merit more detailed investigations.

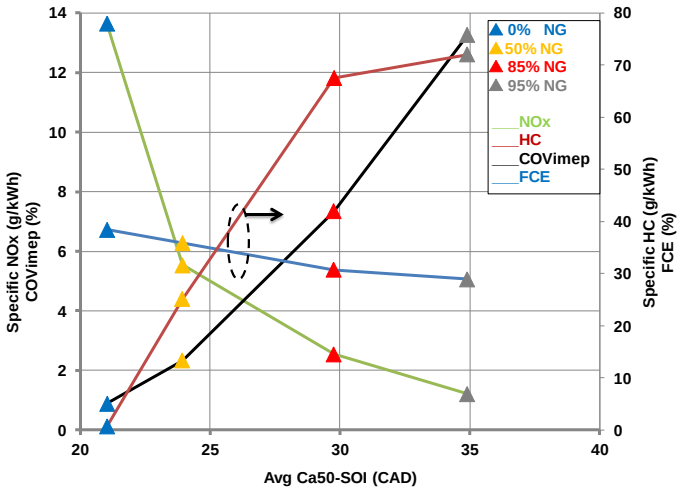

Figure 2: Specific NOx and HC emissions, COVimep and FCE vs. relative combustion phasing for conventional dual fuel combustion

Figure 3 shows the magnitude of maximum cylinder pressure (Pmax) and Ca50 versus the location of maximum cylinder pressure (CaPmax) in CAD for various NG substitutions. The motivation for this plot is a similar representation in a seminal paper on the nature of cyclic combustion variations in spark ignition engines by Matekunas [12]. Matekunas states that cyclic combustion variations in SI engines are characterized by the presence of fast and slow burn cycles. Fast burn cycles are characterized by higher Pmax magnitudes and CaPmax phased away from TDC, while slow burn cycles are characterized by lower Pmax magnitudes and CaPmax phased closer to TDC. He also mentions that Pmax and CaPmax should be used in conjunction with Ca50 to completely understand the nature of cyclic fluctuations.

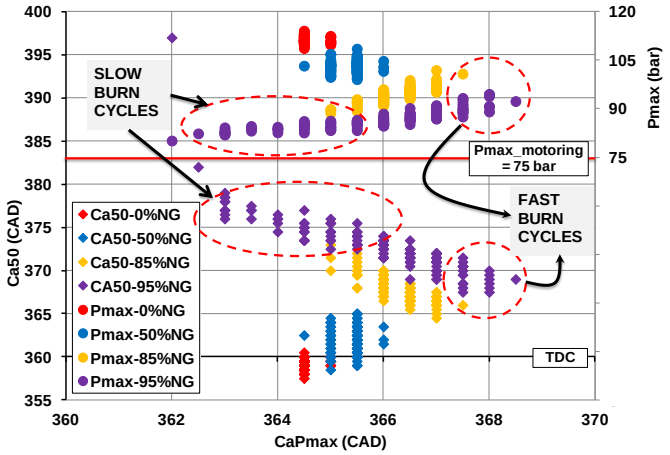

Figure 3: Pmax vs. CaPmax for conventional dual fuel combustion

We have attempted to develop Matekunas' idea further in Fig. 3 relative to dual fuel combustion. With increasing NG substitution, the following observations can be made: the overall magnitude of Pmax is observed to decrease, the variability in CaPmax and Ca50 increases, and finally, the average Ca50 is phased away from TDC. Also, at any given NG substitution (say 95%NG), there are clear "slow burn" and "fast burn" cycles. It is instructive to point out that as NG substitution increases, the pilot injection is increasingly separated from the combustion event. Consistent with Matekunas' observations, for slow burn cycles Pmax magnitudes are lower (really close to maximum motoring pressures), the CaPmax is phased closer to TDC and the Ca50 is phased farther away from TDC. Figure 4, showing Pmax versus Ca50, further corroborates the fact that the Pmax magnitudes decrease and Ca50 is increasingly removed from TDC with increasing NG substitutions. In fact, there is linear (albeit negative) correlation between Pmax and Ca50. These observations collectively account for the decrease in FCEs and increase in COVimep reported in Fig. 2 with increasing NG substitution, particularly at 95% NG.

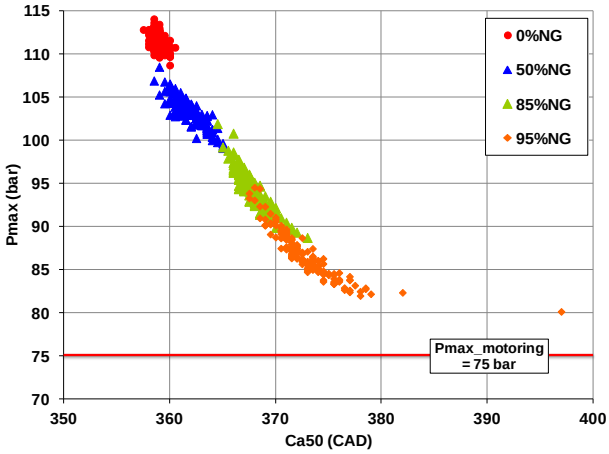

Figure 4: Pmax vs. Ca50 for conventional dual fuel combustion

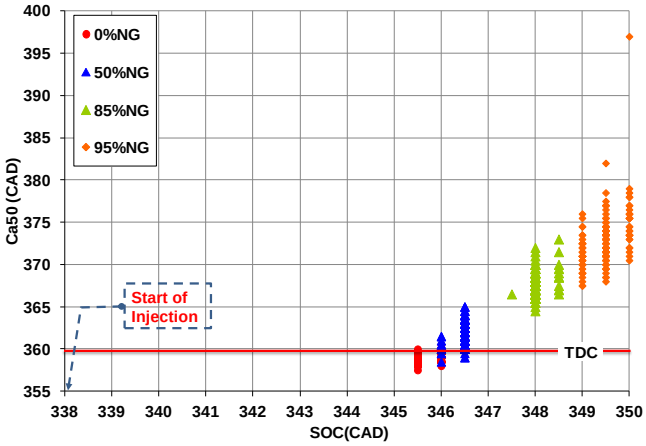

Figure 5: Ca50 vs. SOC for conventional dual fuel combustion

Figure 5 illustrates the cyclic variations in Ca50 versus SOC at various NG substitutions. It is believed that with increasing NG addition in dual fuel engines there is a transition from spray combustion as in straight diesel operation to flame propagation induced by diesel autoignition [5]. Therefore, it is pertinent to examine the nature of this transition with increasing NG substitution. As seen in Fig. 5, at 95% NG, the variability in Ca50 is about 10 CAD, whereas, the variability in SOC is about 1 CAD. As mentioned before, the injection event is separated from the combustion event for this condition. This indicates that the cyclic combustion variations at 95% NG are not caused as much by variability in the diesel autoignition process as the variability in the NG combustion (possibly by flame propagation). It is instructive to note that at this operating condition, the overall equivalence ratio is about 0.4 [3]. Recent numerical investigations by Egolfopoulos et al. [13] show that the lean flammability limit for methane- and propane-air mixtures extend beyond the nominal atmospheric lean limit (Φ = 0.5) at engine-like pressures and temperatures. Therefore, there is some support for the hypothesis that flame propagation can indeed occur in dual fuel engine combustion at substantially leaner conditions than previously believed. Egolfopoulos et al. also suggest that a successful autoignition event should lead to sustained burn in an engine in the absence of extinction caused by turbulence and stretch; however, turbulence and flame stretch are unavoidable in an IC engine. For the present case, as seen in Fig. 5, autoignition is established in each cycle for all NG substitutions, indicating that combustion could be sustained in principle. However, the high cyclic variations in Ca50 may be attributed to post-ignition cyclic variations in the bulk fluid motion, turbulence, and flame stretch that may cause inconsistencies flame propagation from one engine cycle to another. These cyclic variations in Ca50 are manifested as IMEP variations, as evident from the high COVimep values indicated in Fig. 2 (about 12 percent at 95% NG).

Figure 6 shows the first-order heat release return maps for conventional dual fuel combustion at various NG substitutions. The first-order heat release return map is an important tool to understand the nature of cyclic combustion variations. Its use was popularized in studies by Daw and co-workers at Oak Ridge National Laboratory [14-17]. In principle, a return map is used to estimate the degree of cyclic combustion variability from one engine cycle to the next immediate cycle in the future. This information can be used to build feed-forward next-cycle control systems to adjust engine operating parameters such as overall equivalence ratio [14,15] and residual gas fraction [16] to aid in the control of cyclic combustion variations. As seen in Fig. 6, the heat release return maps indicate that for straight diesel fueling (0% NG), the cyclic variations in heat release are relatively small and appear to be stochastic in nature. The return map for 0% NG is very similar to the "time-reversible" fuzzy circular patterns observed for stable, stoichiometric spark ignition (SI) engine operation in Ref. [17]. With increasing NG addition, particularly at 95% NG, there is evidence of alternating slow burn cycles, characterized by smaller magnitudes of normalized heat release, and fast burn cycles, characterized by larger magnitudes of normalized heat release. This indicates that prior cycle effects are communicated to subsequent cycles at high NG substitutions, rendering the cyclic combustion variations more "time irreversible and deterministic" compared to 0% NG. The impact of such prior cycle effects on lean burn SI engine combustion was investigated in Refs. [17] and [18]. For 95% NG, the onset of instability results in occasional partial misfiring cycles (characterized by lower heat release) that are manifested as "arms" in the return map. Similar asymmetric arms, indicative of time-irreversibility, were also observed in Ref. [17] with SI engines operating at lean equivalence ratios (~ 0.72). This behavior lends itself to adaptive control strategies similar to those discussed in Wagner et al. [15] and Edwards et al. [16]. Although the control algorithms were demonstrated on lean burn natural gas fired SI engines in their studies, the principle can be extended to control dual fuel combustion at high NG

substitutions since it exhibits cyclic heat release fluctuations similar to lean operation of SI natural gas engines [16].

3.2. Partially Premixed Dual Fuel LTC

For the partially premixed dual fuel low temperature combustion (LTC) experiments, very small diesel quantities were employed and the SOI of the pilot diesel fuel was varied from 20° to 60°BTDC. As mentioned in the experimental section, the pilot quantity was fixed at 3.3 g/min for the entire LTC experimental matrix. The diesel injection system was operated using an externally powered motor and the engine brake power was not corrected to account for the externally powered injection system or for the power expended in obtaining compressed, preheated intake air. For the SOI sweep from 20°BTDC to 60°BTDC, NG fueling was appropriately adjusted to maintain a constant BMEP of 6 bar.

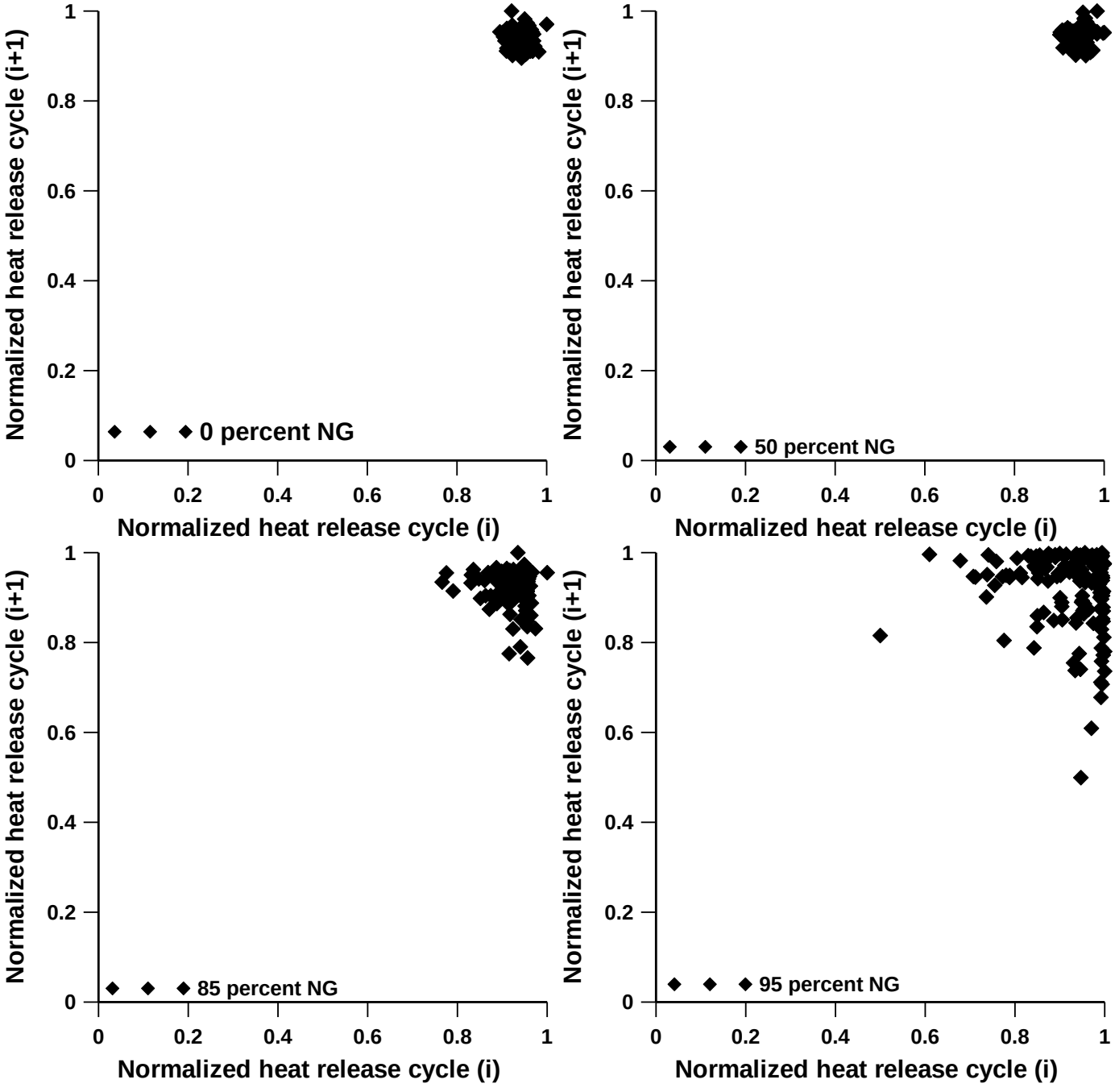

Figure 6: Normalized first-order heat release return maps for various % NG substitutions for conventional dual fuel combustion

Figure 7 shows the brake specific NOx, brake specific HC, FCE, and COVimep versus the relative combustion phasing for half load operation for partially premixed diesel-ignited natural gas LTC (ALPING combustion). These quantities are plotted against the relative combustion phasing (which quantifies the separation of the combustion event from the SOI) to elucidate the influence of the relative combustion phasing on ALPING combustion and emissions. For example, engine-out NOx emissions first increase from 0.4 g/kWh to 1.2 g/kWh as SOI is advanced from 20° to 30°BTDC and then progressively decrease with further SOI advancement to 0.02 g/kWh at 60°BTDC, which is well below the 2010 statute for heavy duty diesel engines.

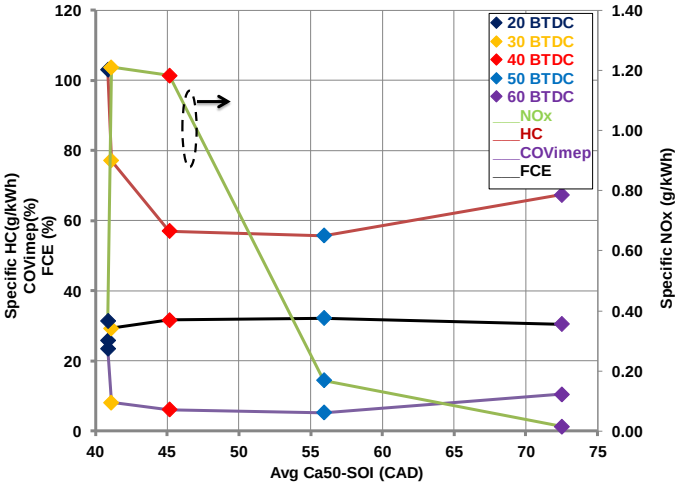

Figure 7: Specific NOx and HC emissions, COVimep and FCE vs. relative combustion phasing for dual fuel LTC

The separation of Ca50 from SOI, the SOI, and the phasing of Ca50 with respect to TDC have a profound influence on NOx emissions. As evident from Fig. 8, when the SOI is advanced from 20° to 40°BTDC, the SOC is advanced by about 10 CAD; further advancement in SOI leads to a more retarded SOC, with 60°BTDC having SOC values very similar to 20°BTDC. This swing in SOC, when combined with the trends observed for Ca50 and relative combustion phasing, sheds more light on the combustion parameters that have the most impact on NOx emissions as SOI is varied. For example, while 30°BTDC and 50°BTDC SOIs have roughly the same average SOC, the NOx emissions are extremely different. In fact, the highest NOx emissions were obtained at the SOI of 30°BTDC, despite the fact that the average Ca50 for this SOI was actually slightly more retarded with respect to TDC compared to 50°BTDC. A similar comparison can be made between 20°BTDC and 60°BTDC SOIs, with the additional observation that the average Ca50 was considerably more retarded for 20°BTDC, and yet, the NOx emissions were lowest for 60°BTDC. To explain these somewhat counterintuitive trends of higher NOx emissions for the more retarded Ca50 values, it is useful to examine the relative combustion phasing behavior.

As SOI is advanced from 20°BTDC, the relative combustion phasing remains approximately constant until 30°BTDC but increases rapidly thereafter. Thus, while 30°BTDC and 50°BTDC have similar SOCs and Ca50s, the relative combustion phasing is roughly 15 CAD higher for the earlier SOI. This difference in relative combustion phasing is even more pronounced (~ 30 CAD) between 20°BTDC and 60°BTDC. Higher relative combustion phasing implies that the combustion event occurs farther away from the pilot injection event, and therefore, the pilot diesel fuel will be more premixed with the surrounding lean NG-air mixture at the time of combustion. For constant SOC and Ca50, the more stratified the overall combustion process, the higher are the local temperatures, and therefore, higher the NOx emissions. Thus, there is a balance between SOC, Ca50, and relative combustion phasing vis-à-vis their effects on NOx, HC, FCE, and COVimep.

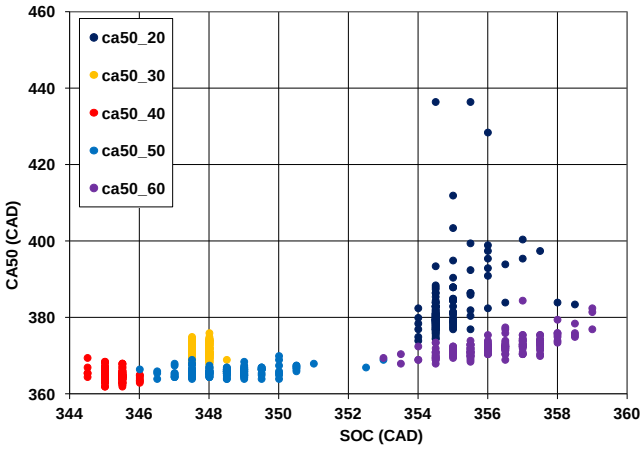

Figure 7: Ca50 vs. SOC for dual fuel LTC

Figure 7 also shows that the HC emissions decrease from about 105 g/kWh to 58 g/kWh with SOI advancement from 20° to 40°BTDC and then increase to 70 g/Kwh with further SOI advancement to 60°BTDC. These trends are consistent with the trends observed for Ca50 and relative combustion phasing. Since the earliest SOC and the most conducive Ca50 (closest to TDC) were obtained at 40°BTDC, the lowest HC emissions were obtained at this SOI. By comparison, for 20°BTDC, the highly retarded Ca50 values coupled with excessive cyclic variations in Ca50 led to incomplete combustion events and the highest HC emissions. On the other hand, the high relative combustion phasing for 60°BTDC led to greater mixing of diesel with the lean NG-air mixture (and possibly some spray impingement on cylinder walls), thus increasing HC emissions. The COVimep is highest at 20°BTDC (nearly 25 percent) and progressively decreases (to 6 percent) with SOI advancement to 40°BTDC and increases again to 10 percent with further advancement to 60°BTDC. The COVimep trends, especially for 20°BTDC and 60°BTDC, are also consistent with the

observed cyclic variations in SOC and Ca50. The main difference is that SOC variations appear slightly more significant for 60°BTDC while Ca50 variations are the primary cause of cyclic variations for 20°BTDC. Finally, the FCE is about 26 percent at 20°BTDC, increases to about 31.5 percent as SOI is advanced to 40°BTDC, and decreases slightly to 30 percent as SOI is advanced further to 60°BTDC. These results are also consistent with the Ca50 trends: the closer the phasing of the combustion process to TDC, the higher the FCE.

Figure 9 shows Pmax and Ca50 versus CaPmax for dual fuel LTC at different SOIs. The lowest Pmax and the most retarded Ca50 values can be observed at 20°BTDC. By comparison, 40°BTDC exhibited the highest Pmax values and Ca50 values closest to TDC. At 60°BTDC, the Pmax values are lower compared to 40°BTDC, CaPmax is between 364 and 371 CAD, and Ca50 is phased closer to TDC compared to 20°BTDC. When SOI is advanced from 20°BTDC, the CaPmax is generally retarded away from the TDC, but at 40°BTDC, there is "hook-back" where the CaPmax is located closer to the TDC and further SOI advancement to 60°BTDC moves the CaPmax farther away from TDC.

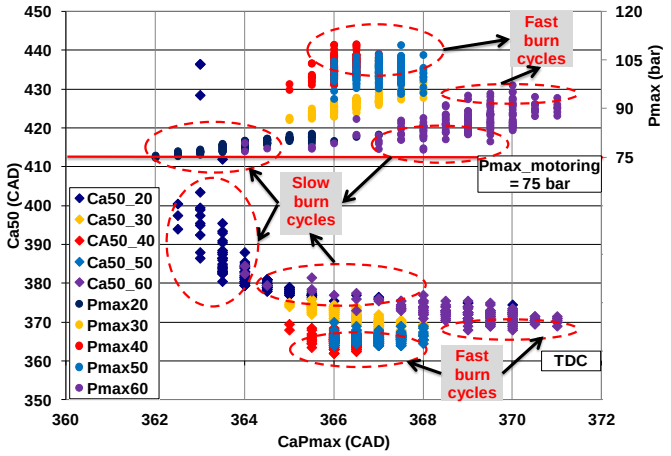

Figure 8: Pmax and Ca50 vs. CaPmax for dual fuel LTC

These observations reinforce the fact that there are variations in both the magnitude and phasing of Pmax across SOIs and also between cycles for a given SOI. In other words, there are "slow burn" and "fast burn" cycles across SOIs and within a given SOI as indicated in Fig. 9. For instance, at 20°BTDC, the Ca50 is located farthest away from TDC and therefore the overall combustion rates are generally low, resulting in the lowest FCE. At 40°BTDC, the Ca50 is phased closest to the TDC and the combustion rates are the fastest among the range of investigated SOIs, leading to the highest FCE value. At 60°BTDC, the Ca50 is generally between the values observed at 20° and 40°BTDC and the FCE is slightly lower than at 40°BTDC, indicating that the combustion rates are faster than at 20°BTDC.

Within SOIs, particularly at 60°BTDC, there are clearly both fast and slow burn cycles. The slow burn cycles are characterized by lower Pmax magnitudes, CaPmax phased closer to TDC, and Ca50 phased farther away from TDC. The fast burn cycles are characterized by high Pmax, CaPmax phased away from TDC and Ca50 phased closer to TDC. This indicates that as SOI is advanced, the nature of combustion changes significantly, and is characterized by high cyclic fluctuations. There is evidence of slow burn cycles followed by fast burn or recovery cycles. This is probably related to the fact that since the pilot diesel injection event is considerably separated from the combustion event, there might be overmixing of the injected diesel in some cycles. As a result, there might be fewer distributed ignition sites, and hence slower overall combustion rates. Whereas in the fast burn cycles, the injected diesel may be premixed "just enough" to attain sustained ignition; thereby, resulting in overall faster combustion rates. These observations indicate that the post-injection mixing process is crucial to obtaining repeatable combustion from one engine cycle to another.

Figure 10 is a plot of Pmax versus Ca50 for SOIs between 20° and 60°BTDC. The Pmax vs. Ca50 trends are almost linear at all SOIs with almost similar overall slopes, except at 20°BTDC. The negative linear correlation between Pmax and Ca50 at different SOIs is similar to a similar trend observed with increasing %NG in Fig. 4. In general, the Ca50 for most SOIs is phased between 360 and 380 CAD with the exception of 20°BTDC, where the Ca50 phasing ranges from 375 – 400 CAD, with some cycles phased as late as 440 CAD.

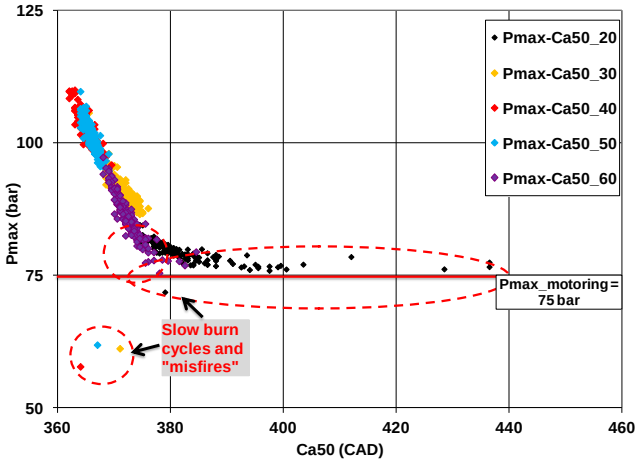

Figure 9: Pmax vs. Ca50 for dual fuel LTC

Clearly at any SOI, slow burn cycles are characterized by low Pmax and later combustion phasing. This is evident at 20° and 60°BTDC. In addition, there are some misfiring cycles (outlier data points), indicated by Pmax less than the maximum motoring pressures. In general, it can be seen that advancing the SOI from 20°BTDC results in overall faster burn rates, especially at 40°BTDC, and any further SOI advancement beyond 40°BTDC tends to reverse the trend, i.e., the combustion rates are reduced again. The late Ca50 and lower

Pmax explain the low FCE values and high HC emissions at 20°BTDC and the large variability in Ca50 results in high COVimep. At 60°BTDC, on the other hand, the variations in Ca50 are reflected in relatively lower COVimep values, and the presence of slow burn cycles due to late combustion phasing accounts for high HC emissions. The Pmax values exhibit considerable variation, resulting in slightly compromised FCE compared to 40°BTDC.

Figure 11 shows Pmax versus the relative combustion phasing for different SOIs from 20° to 60°BTDC. In addition, FCE and HC emissions are also plotted against the relative combustion phasing. This plot shows the relevance of the relative combustion phasing for dual fuel LTC. As discussed before, larger magnitudes of the relative combustion phasing indicate that the injection and combustion event are significantly separated. From Fig. 11, it is evident that the relative combustion phasing affects Pmax significantly, both across SOIs and within a given SOI. For instance, it can be seen that the magnitude of Pmax for all cycles at a given SOI tends to increase with advancing SOI up to 40°BTDC and then decrease with further advancement to 60°BTDC. It is also seen that the FCE and HC trends mirror one another; as FCE increases, HC decreases. Interestingly, they are correlated with the Pmax behavior at different relative combustion phasings. For example, the FCE increases and the HC emissions decrease as the SOI is advanced to 40°BTDC, where the Pmax values also peak. Further advancement of the SOI decreases Pmax and FCE and leads to a more modest increase in HC emissions. The HC emissions are highest for 20°BTDC, which shows high cyclic variability in the relative combustion phasing and the lowest Pmax values.

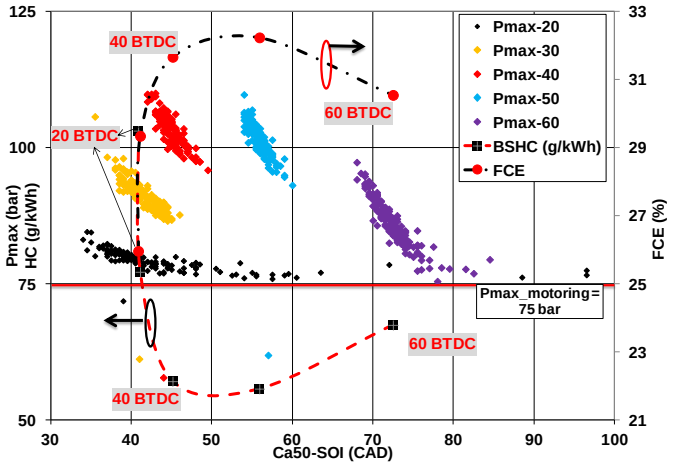

Figure 10: Pmax, HC, and FCE vs. relative combustion phasing for dual fuel LTC

It is clear that the lower Pmax and the slower combustion rates for 20°BTDC result in lower local temperatures and incomplete HC oxidation. By contrast, for 40°BTDC SOI, the combustion rates are faster, resulting in higher FCE, higher local temperatures, lower HC, and higher Pmax. An additional fact that is evident at all SOIs is that the lower the relative combustion phasing (i.e., the closer the combustion event is to the injection event) for a given engine cycle, the higher the corresponding Pmax value. The slope of this correlation between Pmax and relative combustion phasing appears to have a direct impact on the observed FCE trends. At 60°BTDC SOI, despite the higher average relative combustion phasing, the Pmax values are higher than for 20°BTDC SOI, leading to higher FCE for the more advanced SOI.

Figures 12 - 14 show the first order heat release return maps at 20°, 40°and 60°BTDC SOIs for 75°C and 105°C intake temperatures. At T_{in} = 75°C, the heat release return maps show considerable cyclic combustion fluctuations at 20° and 60°BTDC relative to 40°BTDC. This is evident from the large scatter in the heat release from one cycle to another. Srinivasan et al. [19,20] investigated intake charge heating, intake pressure boosting, increasing pilot diesel quantity, and uncooled EGR as possible thermal management strategies to improve the overall low load performance of dual fuel LTC. From Figs. 12 - 14, it is evident that intake charge heating from 75°C to 105°C significantly improves cyclic combustion fluctuations for all SOIs. This is evident from the considerable reduction in scatter in the heat release return maps at higher intake temperatures. In addition, Table 2 shows that FCE, HC and COVimep are benefited from intake charge preheating; however, with modest NOx penalty. For example, at the most advanced SOI of 60°BTDC, the NOx emissions increase to 0.12 g/kWh at 105°C, which is still well below the 2010 heavy duty NOx standards.

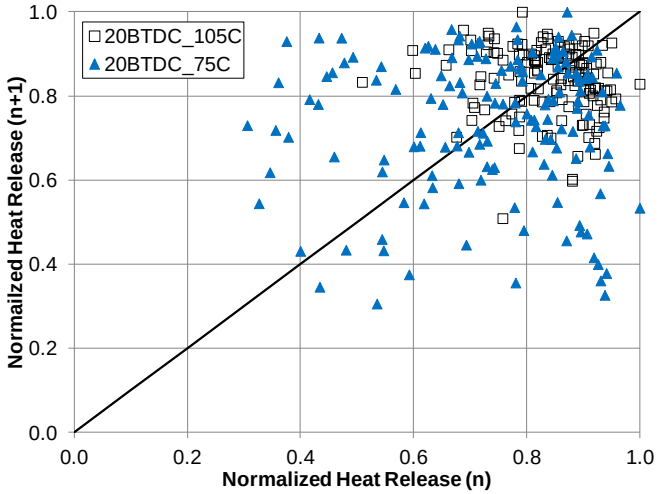

Figure 11: Normalized heat release return map for dual fuel LTC with 20°BTDC SOI and T_{in} = 75°C and 105°C

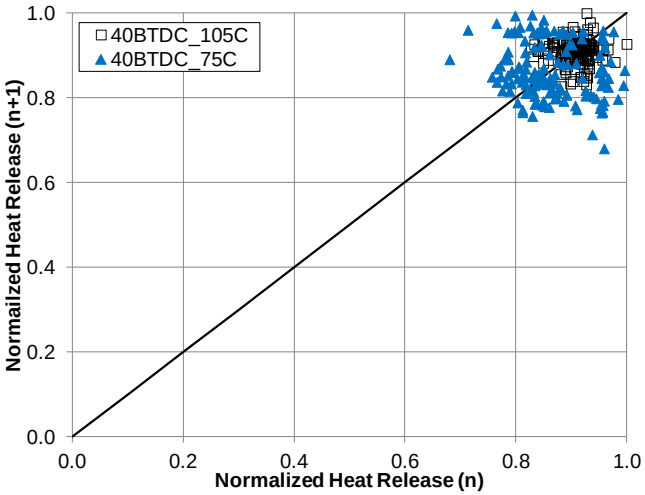

Figure 12: Normalized heat release return map for dual fuel LTC with 40°BTDC SOI and T_{in} = 75°C and 105°C

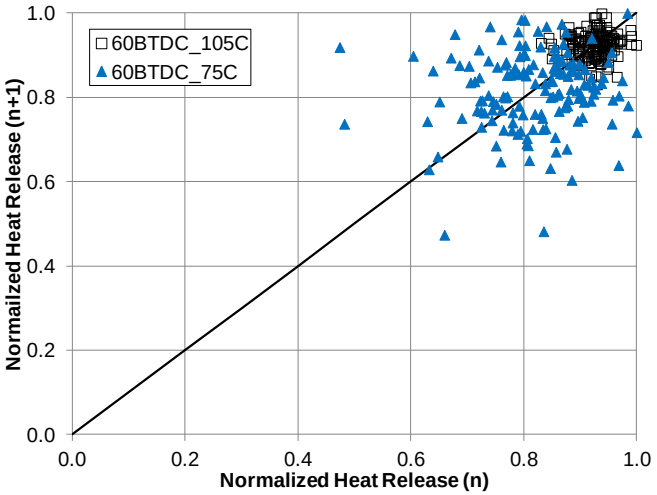

Figure 13: Normalized heat release return map for dual fuel LTC with 60°BTDC SOI and T_{in} = 75°C and 105°C

Table 2: Effects of T_{in} on ALPING LTC at BMEP = 6 bar

SOI	FCE		COVimep		HC		NOx	
°BTDC	%		%		g/kWh		g/kWh	
	75 °C	105 °C	75 °C	105 °C	75 °C	105 °C	75 °C	105 °C
20	26	29.5	23.6	11.6	103.1	58.3	0.37	0.68
40	31.6	37.3	6.2	3.3	57.1	18.3	1.18	2.14
60	30.5	38	10.6	3.8	67.4	18	0.02	0.12

4. CONCLUSIONS

Conventional dual fuel (diesel-ignited natural gas) and dual fuel partially premixed low temperature combustion (LTC) experiments were performed on a single cylinder research engine. For the conventional dual fuel experiments, the pilot diesel was injected using a mechanical injection system with fixed injection timing (22°BTDC) throughout the experimental program and natural gas fueling was varied between 0 and 95 percent on an energy basis. For the partially premixed dual fuel LTC experiments, the pilot diesel injection was accomplished using a custom-built, electronic injection system. Pilot injection timing (SOI) was varied between 20° and 60°BTDC while pilot quantity was fixed at 3.3 g/min, accounting for about 2 percent of the injected energy. Natural gas was fumigated into the intake manifold and accounted for about 98 percent of the total energy. For both experimental programs, the intake temperature was maintained a constant at 75°C, the intake pressure was maintained at 181 kPa and the exhaust pressure was maintained at 171 kPa. The engine speed was maintained at 1700 rev/min. The brake power of the engine was maintained constant at 21 kW (BMEP = 6 bar). Additional experiments were performed for the partially premixed dual fuel LTC program, where intake air was preheated to 105°C as a means to improve cyclic combustion variations and reduce engine-out hydrocarbon (HC) emissions. The following are the salient conclusions from these experimental investigations.

1. Conventional Dual Fuel Combustion

1.1. Brake specific NOx emissions decreased by 90 percent at 95% NG relative to straight diesel operation (0% NG). The reduction in NOx emissions is likely due to a combination of two phenomena: (i) reduction in pilot diesel sizes and (ii) the separation of the diesel pilot injection event from the overall combustion process as quantified by the relative combustion phasing (Ca50 – SOI).

1.2. Brake specific HC emissions increased by 98 percent at 95% NG compared to 0% NG. This increase is due delayed relative combustion phasing, slower combustion rates, and lower bulk gas temperatures. For the same reasons, fuel conversion efficiency (FCE) was lower by about 10 percentage points at 95% NG compared to 0% NG.

1.3. Coefficient of variation of indicated mean effective pressure (COVimep) increased by nearly 12 percentage points at 95% NG relative to 0% NG. These cyclic variations are related to the occurrence of "fast burn" and "slow burn" cycles at 95% NG as evident from correlations between maximum cycle pressures (Pmax), the location of Pmax (CaPmax), and the relative combustion phasing.

1.4. As % NG is increased, Pmax decreases, SOC and Ca50 are delayed (Ca50 is farther away from TDC), and cyclic combustion variations are increased. A linear, negative correlation was observed between Pmax and Ca50 in all engine cycles for all %NG.

1.5. First-order heat release return maps were plotted and the results indicated that cyclic combustion variability is minimal but stochastic in nature for 0% NG, while 95% NG showed more intense, deterministic cyclic variations.

2. Dual Fuel Partially Premixed LTC

2.1. Brake specific NOx emissions decreased by 95 percent at 60°BTDC relative to 20°BTDC. At 60°BTDC the injected diesel has a higher residence time to mix with the surrounding lean NG-air mixture as evidenced by a large relative combustion phasing. As a result, the ensuing combustion results in low local temperatures and a consequent reduction in NOx emissions.

2.2. Brake specific HC emissions are 103.1 g/kWh at 20°BTDC and decrease with advancing SOI up to 55.6 g/kWh at 50°BTDC, but increase again to 67.4 g/kWh at 60°BTDC. Similarly, FCE increased from 25.3 percent at 20°BTDC to 31.6 percent at 40°BTDC and then decreased back to 30.5 percent at 60°BTDC. This swing in HC emissions and FCE is attributed to retarded Ca50, and low Pmax magnitudes at 20°BTDC and to alternating "slow" and "fast" burn cycles at 60°BTDC. At 40°BTDC, Ca50 is located closer to TDC, indicating faster burn rates and better utilization of the expansion volume, both resulting in improved HC emissions and higher FCEs.

2.3. COVimep decreased from nearly 25 percent at 20°BTDC to 6.2 percent at 40°BTDC and increased back up to 10.6 percent at 60°BTDC. At 20°BTDC, the large cyclic combustion variations in Ca50 are reflected in cyclic variations in work output. At 60°BTDC, the alternating fast and slow burn cycles result in variations in the cyclic work output. At 40°BTDC, the variations in work output are minimal because of smaller variations in Ca50 and faster combustion rates.

2.4. As SOI is advanced from 20° to 60°BTDC, Pmax first increases and reaches a maximum at 40°BTDC and then decreases at 60°BTDC. At the same time, the relative combustion phasing increases in magnitude with SOI advance from 20° to 50°BTDC. This swing in Pmax values along with the relative combustion phasing trends are well correlated with both FCE and HC trends.

2.5. Cycles with higher Pmax, CaPmax phased away from TDC and Ca50 phased closer to TDC are fast burn cycles, while cycles with lower Pmax, CaPmax phased closer to TDC and Ca50 retarded away from TDC are slow burn cycles. Pmax, CaPmax and Ca50 were identified as important measures to understand the nature of cyclic combustion variations in dual fuel engines.

2.6. First order heat release return maps were plotted at 20°, 40° and 60°BTDC for intake temperatures of 75°C and 105°C. It is established that intake charge preheating can be used as a possible thermal management strategy to improve cyclic combustion fluctuations.

5. ACKNOWLEDGMENTS

The authors gratefully acknowledge financial support the US Department of Energy (Award # DE-FG36-06GO86025). The views and opinions expressed herein are not necessarily those of the sponsoring agency or the university.

6. REFERENCES

1 Karim, G. A. 1987 The dual fuel engine. In *Automotive Engine Alternatives* Ed. R. L. Evans Plenum Press.

2 Gibson, C. M., Polk, A. C., Shoemaker, N. T., Srinivasan, K. K., Krishnan, S. R. 2011 Comparison of Propane and Methane Performance and Emissions in a Turbocharged Direct Injection Dual Fuel Engine. Vol. 133, 9.

3 Krishnan, S. R., Biruduganti, M., Mo, Y., Bell, S. R., Midkiff, K. C. (2002). Performance and heat release analysis of a pilot-ignited natural gas engine. International Journal of Engine Research, 3(3), 171-184.

4 Papagiannakis, R. G., and Hountalas, D. T., 2003, "Experimental Investigation of Natural Gas Percentage on Performance and Emissions of a D.I. Dual Fuel Engine," Appl. Therm. Eng., 23, pp. 353–365.

5 Karim, G. A. 2003 Combustion in Gas Fueled Compression: Ignition Engines of the Dual Fuel Type. Transactions of the ASME: Journal of Engineering for Gas Turbines and Power, Vol. 125, 827-836

6 Gebert, K., Beck, N. J., Barkhimer, R. L., and Wong, H. C. (1997) Strategies to Improve Combustion and Emission Characteristics of Dual-Fuel Pilot Ignited Natural Gas Engines, SAE Paper No. 971712.

7 S. R. Krishnan, K. K. Srinivasan, S. Singh, S. R. Bell, K. C. Midkiff, W. Gong, S. B. Fiveland, M. Willi, 2004, "Strategies for Reduced NOx Emissions in Pilot-Ignited Natural Gas Engines," *Journal of Engineering for Gas Turbines and Power*, Vol. 126, Issue 3, pp.665-671

8 K. K. Srinivasan, S. R. Krishnan, S. Singh, K. C. Midkiff, S. R. Bell, W. Gong, S. B. Fiveland, and M. Willi, 2006, "The Advanced Low Pilot Ignited Natural Gas Engine – A Combustion Analysis," *Journal of Engineering for Gas Turbines and Power*, Vol. 128, Issue 1., pp. 213-218

9 Splitter, D., Hanson, R., Kokjohn, S., and Reitz, R. 2010 Reactivity Controlled Compression Ignition (RCCI) Heavy-Duty Engine Operation at Mid-and High-Loads with Conventional and Alternative Fuels SAE 2011-01-0363

10 Eichmeier, J., Wagner, U., Spicher, U. 2011 "Controlling Gasoline Low Temperature Combustion by Diesel Micropilot Injection," Paper No. ICEF2011-60042, Proceedings of the Fall Technical Meeting of the ASME IC Engines Div. Oct. 2-4, Morgantown, West Virginia, USA

11 Dec., J. 1997, “A Conceptual Model of DI Diesel Combustion Based on Laser-Sheet Imaging,” SAE 970873
12 Matekunas, F. 1983, “Modes and Measures of Cyclic Combustion Variability,” SAE 830337
13 Egolfopoulos, F. N., Holley, A. T., Law, C. K. 2007, “An Assessment of the Lean Flammability Limits of CH_4/Air and C_3H_8/Air Mixtures at Engine-Like Conditions,” Proc. of the Comb. Inst. 31 (2007), pp. 3015-3022
14 Daw, C. S., Kennel, M. B., Finney, C. E. A., Connolly, F. T. 1998, “Observing and Modeling Nonlinear Dynamics in an Internal Combustion Engine,” Phys. Rev. E, 57(3), pp. 2813-2819
15 Wagner, R. M, Daw, C. S., Green, J. B., Jr. 2001, “Low-Order Map Approximations of Lean Cyclic Dispersion in Premixed Spark Ignition Engines,” SAE 2001-01-3559
16 Edwards, D. K., Wagner, R. B. 2004, “Application of Adaptive Control to Reduce Cyclic Dispersion near the Lean Limit in a Small-Scale, Natural Gas Engine,” Paper No. ICEF2004-855, Proceedings of the ASME IC Engines Div. Fall Technical Conference, Longbeach, Ca. Oct. 24-27, 2004.
17 Green, J. B., Jr., Daw, C. S., Armfield, J. S., Finney, C. E. A., Wagner, R. M., Drallmeier, J. A., Kennel, M. B., Durbetaki, P., 1999, “Time Irreversibility and Comparison of Cyclic-Variability Models,” SAE 1999-0100221.
18 Martin, J. K., Plee, S. L., Remboski, D. J. Jr. (1988) Burn modes and prior-cycle effects on cyclic variations in lean-burn spark-ignition combustion, SAE 880201, 1988.
19 K. K. Srinivasan, S. R. Krishnan, K. C. Midkiff, 2006 “Improving low load combustion, stability and emissions in pilot-ignited natural gas engines,” Proceedings of the Institution of Mechanical Engineers, Part D: Journal of Automobile Engineering: Journal of Automobile Engineering, Part D, 220(2), 229-239
20 K.K. Srinivasan, S. R. Krishnan, Y. Qi., H. Yang, K. C. Midkiff, 2007 "Analysis of diesel pilot-ignited natural gas low-temperature combustion with hot exhaust gas recirculation," Combustion Science and Technology, 179(9), 1737-1776